Technical Report No. 32-125

Experimental Investigation of the Forced-Convection and Nucleate-Boiling Heat-Transfer Characteristics of Liquid Ammonia

M. B. Noel

N66 39951

jpl

JET PROPULSION LABORATORY
CALIFORNIA INSTITUTE OF TECHNOLOGY
PASADENA, CALIFORNIA

July 19, 1961

Technical Report No. 32-125

Experimental Investigation of the Forced-Convection and Nucleate-Boiling Heat-Transfer Characteristics of Liquid Ammonia

M. B. Noel

Donald R. Bartz

D. R. Bartz, Chief
Propulsion Research

CONTENTS

TABLES

FIGURES

39951

ABSTRACT

To achieve a safe and effective design for liquid-propellant rocket engines that are to be regeneratively cooled, knowledge of the heat-transfer characteristics of the propellant that is to be used as the coolant is essential. For many propellants, such as ammonia, the upper limit of nucleate boiling must be considered as the practical limit of the cooling capability of a propellant for rocket-engine application. At higher heat fluxes lies the film-boiling region, which requires excessive surface temperatures to accommodate the characteristically low heat-transfer coefficients. The heat-transfer characteristics of commercial-grade anhydrous ammonia have been obtained experimentally by utilizing electrically heated tubes. A total of fifty-five tests were performed, including measurements in the forced-convection nonboiling and forced-convection nucleate-boiling regions. The upper limit of nucleate boiling q_{ul} has been determined for ranges of velocity, pressure, and liquid bulk temperature that include velocities between 0 and 156 ft/sec, pressures between 150 and 1820 psia, and liquid bulk temperatures between 23 and 158°F. The values of q_{ul} varied from 2 to 14 Btu/in.^{2} sec, depending upon the particular flow condition. An interpolation equation is presented that may be used to predict q_{ul} within the ranges of pressure, velocity, and liquid bulk temperature tested.

I. INTRODUCTION

One of the problems facing the liquid-propellant rocket-engine design engineer is the cooling of combustion-chamber and nozzle walls. If conventional nonrefractory metals, such as stainless steel or aluminum, are used for thrust-chamber liners, cooling by radiation to the surroundings is inadequate for most engine operating conditions. Regenerative cooling, which utilizes one of the propellants as a coolant prior to injection, is the most feasible means of maintaining wall temperatures sufficiently low to retain adequate strength of liner materials. The heat fluxes encountered in rocket engines are generally so high that impractically high coolant velocities are required to prevent transition to nucleate boiling (sometimes called local or surface boiling). In the sub-

cooled nucleate-boiling region the liquid coolant is below the saturation temperature and the heat flux is so high that bubbles grow and collapse on the heated surface as the fluid flows along the passage. If, for a particular condition, the coolant bulk temperature, pressure, and velocity are fixed but the local heat flux is increased, the population density of the bubbles increases. At a sufficiently high local heat flux, the bubbles will coalesce to form a vapor film, which induces a high resistance to heat flow through the film thickness; as a result, a large increase in the surface temperature results. This condition is termed film boiling. For many liquid propellants (includ-

ing ammonia), the wall temperature becomes so high in the film-boiling region that stainless steel melts. Consequently, the heat flux at the upper limit of nucleate boiling may be considered as the limiting capability of a liquid propellant to cool a local surface area on a rocket-engine component. Therefore, a knowledge of the heat-transfer characteristics at the upper limit of nucleate boiling for the propellant to be used as a regenerative coolant is essential to achieve a safe and effective rocket-engine design (Ref. 1). Experimental measurements have been made to determine these heat-transfer characteristics of commercial anhydrous ammonia.

II. FORCED-CONVECTION NUCLEATE-BOILING TEST APPARATUS

A schematic diagram of the flow circuit used for the tests is shown in Fig. 1. High-pressure nitrogen gas was used to force the ammonia from the storage tank through the flow system and into the receiver tank. The flow rate

was measured and controlled by the use of a cavitating venturi and regulated nitrogen gas pressure in the supply tank. The desired ammonia bulk temperature at the test-section inlet was obtained either by means of an
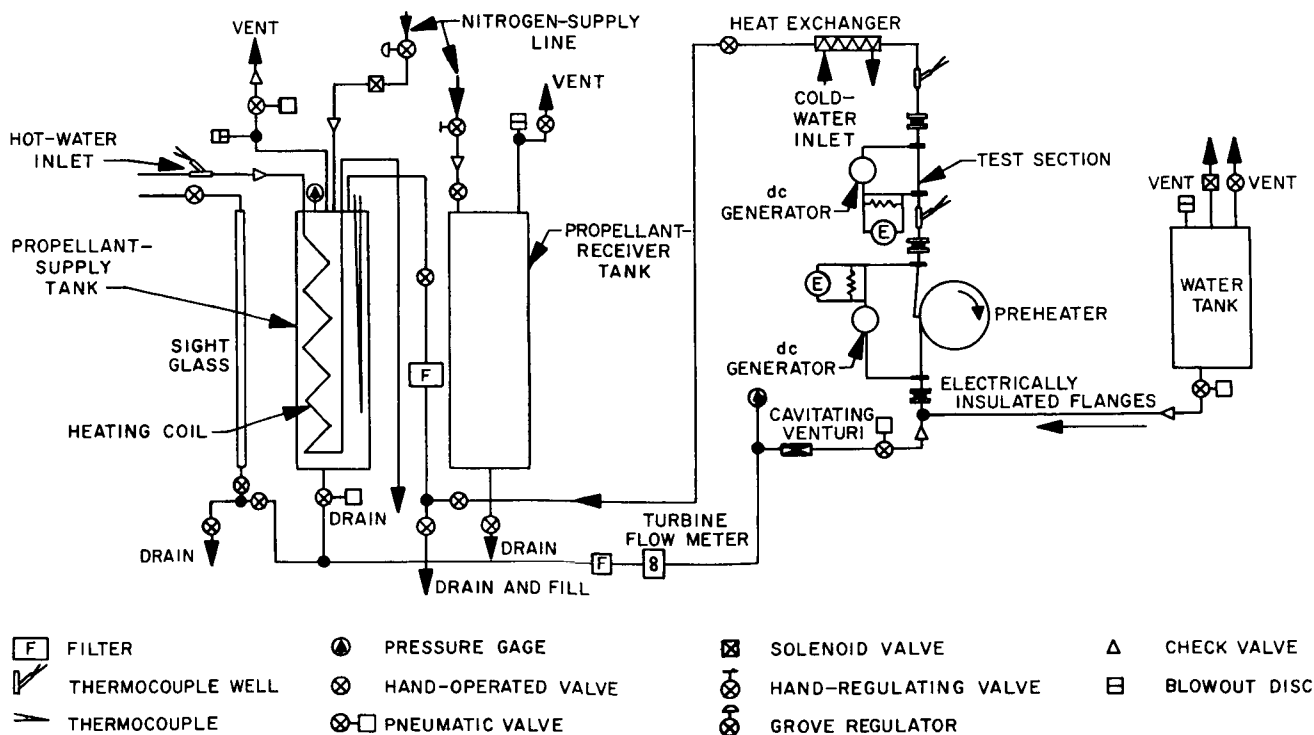
Figure 1. Flow circuit

electrically heated preheater tube or, when cooling was necessary, by precooling the supply tank containing the ammonia.

Two sizes of Type 347 stainless-steel circular tube test sections were used, having dimensions in inches of 0.25 outside diameter, 0.009 wall thickness, and 3.15 length and 0.188 outside diameter, 0.015 wall thickness, and 3.15 length, respectively. An unheated length of tube approxi-

mately 5.8 in. long preceded the heated portion of the test section. The ammonia flowed through the inside of the vertically mounted tubes, and the heat applied to the test section was generated electrically within the tube walls with power supplied by dc welding generators. A more detailed description of the test apparatus and power supply, including tube-wall thickness and electrical resistance measurement techniques, heat losses and accuracies of measurements, is given in Ref. 2.

III. INSTRUMENTATION

Temperature measurements of the outside surface of the test-section tube walls, installed as shown in Fig. 2, were made near the inlet and outlet ends. Liquid bulk-temperature measurements were made at the inlet to and

outlet from the test section. All temperature measurements were obtained with resistance-welded chromel–alumel thermocouples. Tube-wall temperature thermocouples were made of 0.005-in.-diameter wires,
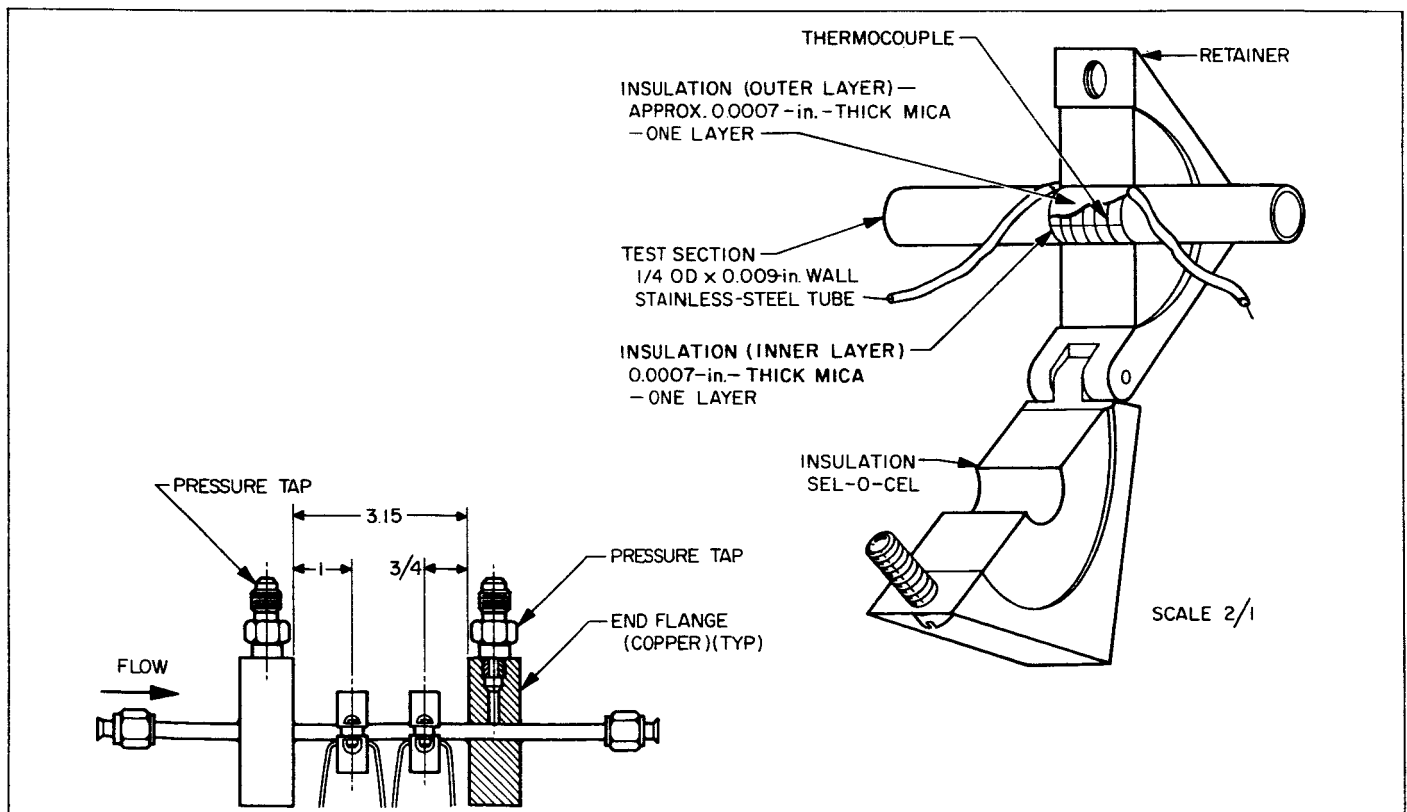
Figure 2. Test-section and wall-thermocouple installation

and liquid bulk-temperature thermocouples, which were fused into the end of a glass tube (Fig. 3), were made of 0.010-in.-diameter wires.

Pressures were measured upstream and downstream of the cavitating venturi so that weight flow rates could be established. A pressure measurement was also made near the outlet of the test section.

Additional information on the details of thermocouple installation and measurement accuracies may be found in Ref. 2.
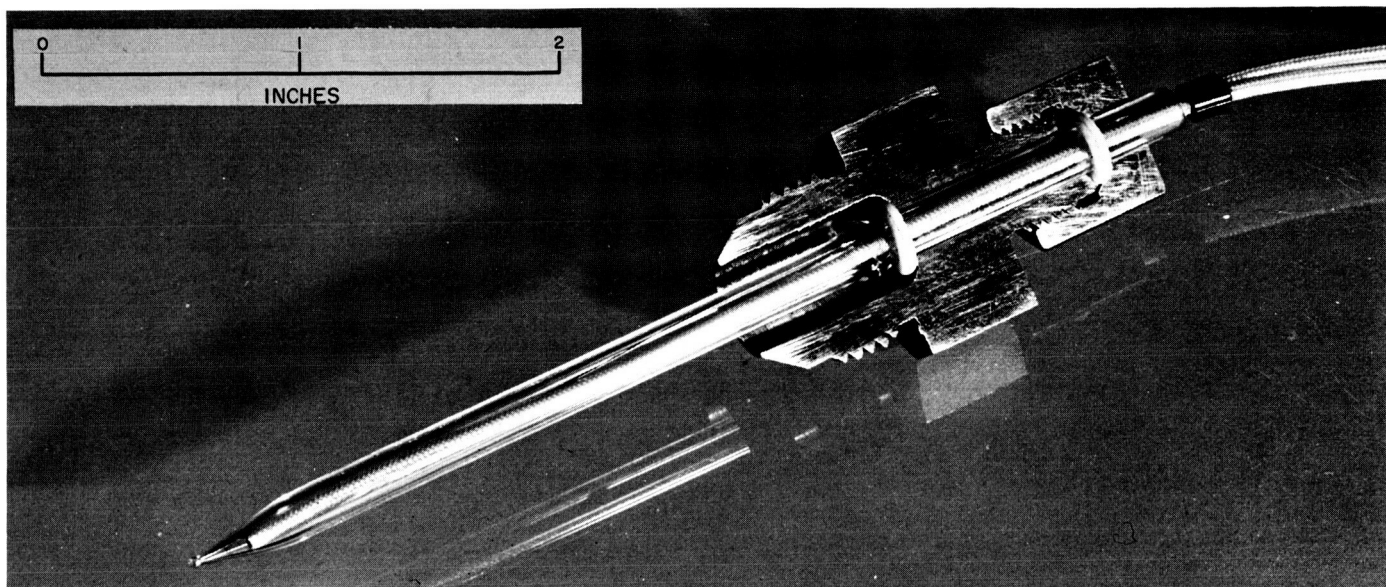
Figure 3. Buik-temperature thermocouple

IV. POOL-BOILING APPARATUS

The tests at zero velocity were performed in a pool-boiling apparatus using a Type 347 stainless-steel strip 0.0043 in. thick, 0.125 in. wide, and 1 in. long, oriented as shown in Fig. 4. The apparatus was essentially a pressure vessel, with an outside jacket enclosing passages which could be used for either cooling or heating the internal liquid. Electrodes through the cover and into the container supplied power to the test strip. A thermocouple also extended through the cover into the liquid so that liquid bulk temperature could be measured.
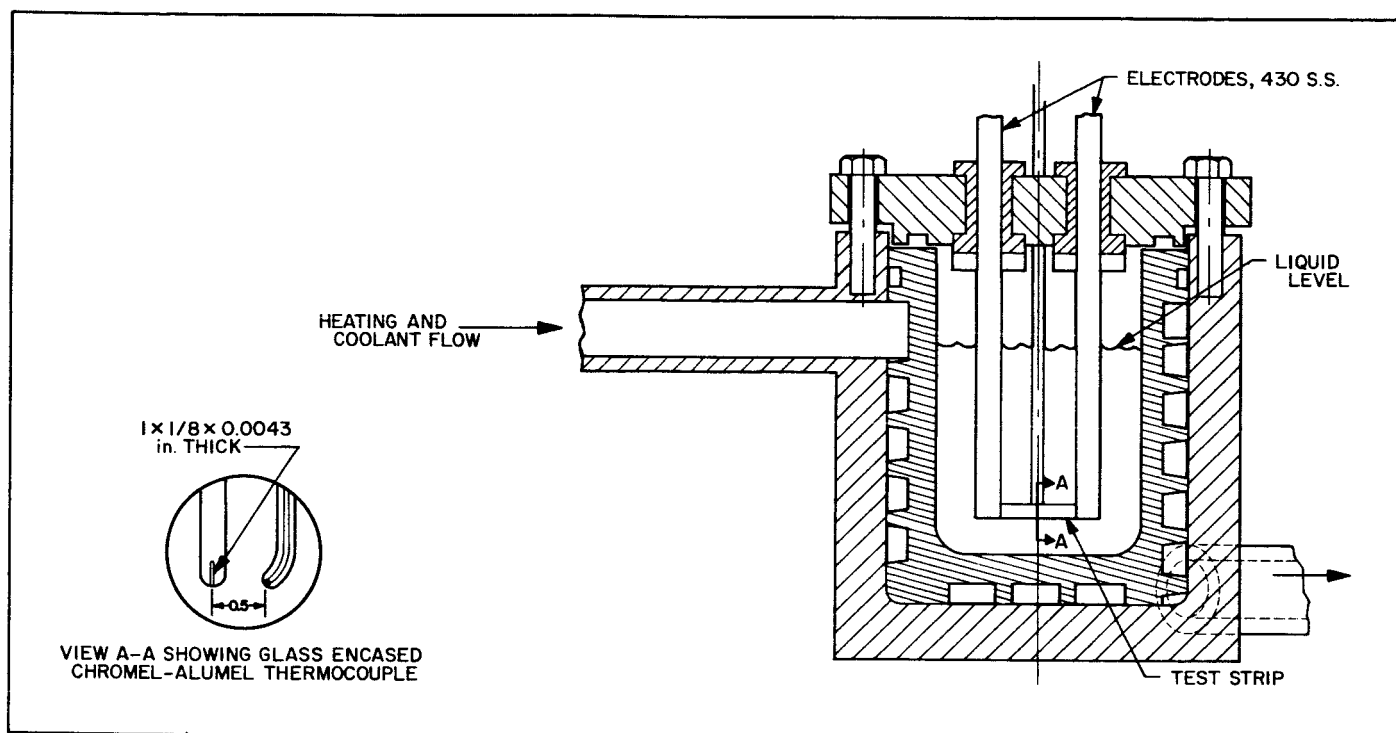
Figure 4. Pool-boiling apparatus

V. DATA COMPUTATION

A. Heat Flux

The electrical power supplied to the test section was used to compute the heat flux from the test section by the equation

$$q = 0.948 \times 10^{-3} \frac{EI}{A_s} \qquad (1)$$

The estimated precision of the value of q determined from Eq. (1) was ±2%. As a check on the electrical measurements of the test-section power, the temperature-dependent resistance R was used to calculate the heat flux, using Eq. (2):

$$q = 0.948 \times 10^{-3} \frac{I^2 R}{A_s} \qquad (2)$$

Resistance R was evaluated at the average wall temperature of the tube (Ref. 2, Fig. 16). The maximum deviation between the values computed from Eqs. (1) and (2) was 5%.

A third method used to compute the heat flux consisted of calculating the heat added to the liquid, using the bulk-temperature rise of the liquid across the test section and the measured weight flow rate.

$$q = \frac{w\, c_p\, \Delta T_b}{A_s} \qquad (3)$$

In general, these results agreed within 5% of those obtained from Eq. (1).

B. Heat Flux at the Upper Limit of Nucleate Boiling

Heat flux at the upper limit of nucleate boiling q_{ul} was calculated from Eq. (1). The values of the current and voltage used in the equation to establish q_{ul} were those measured at the point at which there was a sudden large increase in wall temperature which is characteristic of the transition to film boiling. In nearly all tests, tube failure

occurred simultaneously with this transition. At high bulk temperatures and pressures above 1000 psi there were some tests in which the power could be shut off before tube failure occurred.

C. Liquid-Side Wall Temperature

The liquid-side wall temperature was calculated from the measured outside wall temperature and a theoretical temperature difference across the tube wall which was obtained by assuming uniform internal power generation within the metal wall. The following equation was used for the temperature difference across the tube wall:

$$\Delta T_w = \frac{qr_i}{2k}\left[\frac{4}{\left(\frac{r_i}{r_0}+1\right)^2}-1\right] \tag{4}$$

Values of ΔT_w reached a maximum of 335°F at the highest heat flux measured, which was 14.3 Btu/in.^{2} sec. The thermal conductivity was evaluated at the arithmetic average temperature of the tube wall. A derivation of Eq. (4) is given in Ref. 2.

VI. RESULTS

A. General

The results of the heat-transfer study with subcooled liquid ammonia are presented in Figs. 5 through 11, with emphasis placed upon the values of the heat flux at the upper limit of nucleate boiling q_{ul}. These figures show the effects of pressure, velocity, and liquid bulk temperature on q_{ul}. Some data in the nonboiling forced-convection region were also obtained; the results are shown in Figs. 5 through 8. The ranges of test conditions include pressures between 150 and 1820 psia, velocities between 0 and 156 ft/sec, and liquid bulk temperatures between 23 and 158°F.

B. Nonboiling Region

Figure 5 indicates typical trends of heat flux vs temperature difference between the wall and the liquid. The nonboiling region is represented by the lower straight line having a slope of 45 deg. In this region heat-transfer coefficients h were computed from the equation

$$h = \frac{q}{(T_{wi} - T_b)} \tag{5}$$

where q was evaluated using Eq. (1), T_b was measured, and T_{wi} was computed using Eq. (4) and measured values of T_{wo}. In Fig. 6 comparisons of the experimental values of h obtained in this manner in terms of the Nusselt num-

ber are compared with the following Sieder–Tate correlation equation (Ref. 3):

$$\frac{hD_i}{k_b} = 0.027\left(\frac{\rho_b D_i V}{\mu_b}\right)^{0.8}\left(\frac{\mu c_p}{k}\right)_b^{1/3}\left(\frac{\mu_b}{\mu_{wi}}\right)^{0.14} \tag{6}$$

Curves of viscosity, specific gravity, and specific heat as functions of temperature are shown in Figs. 12, 13, and 14. In Fig. 15 the thermal conductivity is shown as a function of temperature calculated from the following equation (obtained from Ref. 4), which is stated to apply for non-metallic liquids:

$$k = 0.00266 + \frac{(c_p - 0.45)^3}{0.641} + \frac{\left(\frac{S}{M}\right)^{1/3}}{3.31} + \frac{\left(\frac{\mu}{S}\right)^{1/9}}{41.3} \tag{7}$$

where S is the specific gravity, M is the molecular weight, μ is the viscosity in centipoises, and k is the thermal conductivity in Btu/hr ft °F. In Ref. 5 a value of 0.29 Btu/hr ft °F is given for the thermal conductivity of liquid ammonia between 5 to 86°F. This value of k is the same as that predicted by Eq. (7) at 46°F.

Most of the experimental results lie within 20% of Eq. (6), which is typical of forced-convection nonboiling heat-transfer measurements. The hydraulic entrance length-to-diameter ratio upstream of the heated portion of the test-section tube was 25 for the 0.250-in.-diameter tubes
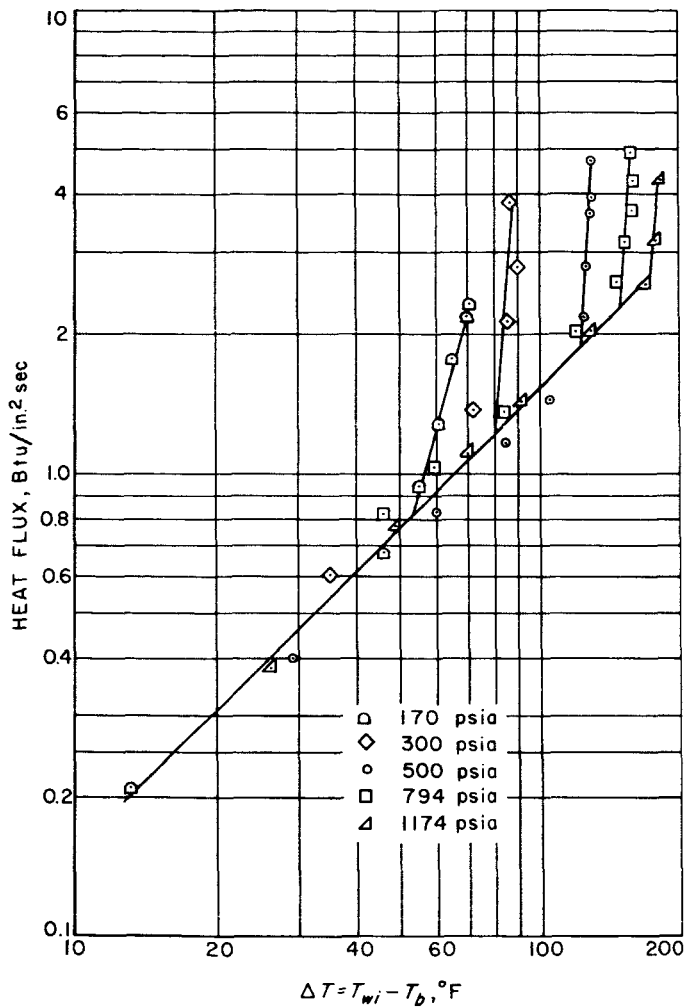
Figure 5. Heat flux as a function of temperature difference for various pressures with constant velocity and bulk temperature

and 37 for the 0.1875-in.-diameter tubes. These lengths are considered adequate to establish fully developed adiabatic flow conditions. Heated length-to-diameter ratios at the outlets of the tubes were 13.6 for the 0.250-in.-diameter tubes and 20.0 for the 0.1875-in.-diameter tubes. Based on the results of Ref. 6, these length-to-diameter ratios are considered adequate to eliminate thermal entrance effects. The wall temperatures and heat-transfer coefficients refer to values near the tube outlets.

C. Nucleate-Boiling Region

The inception of nucleate boiling can be determined from the inside wall temperature. It will be observed that the inside wall temperature increases on the nonboiling curves of Figs. 5, 7, and 8 as heat flux is increased. When
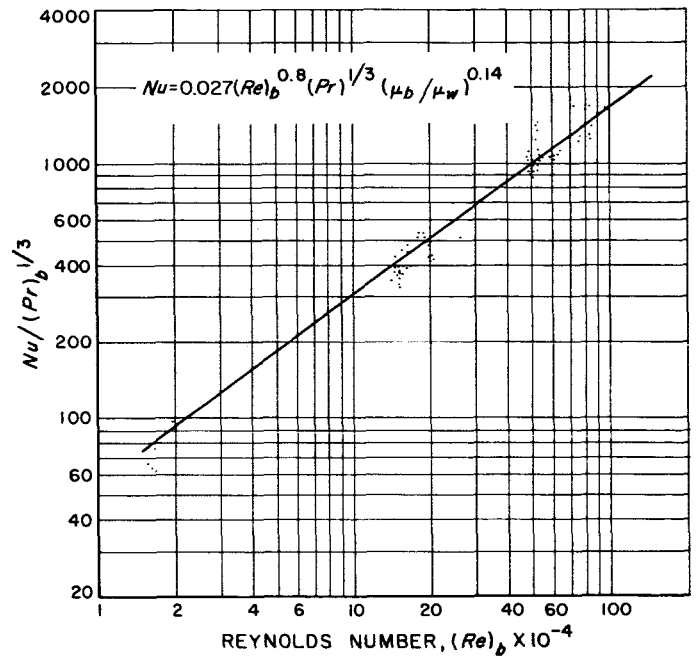

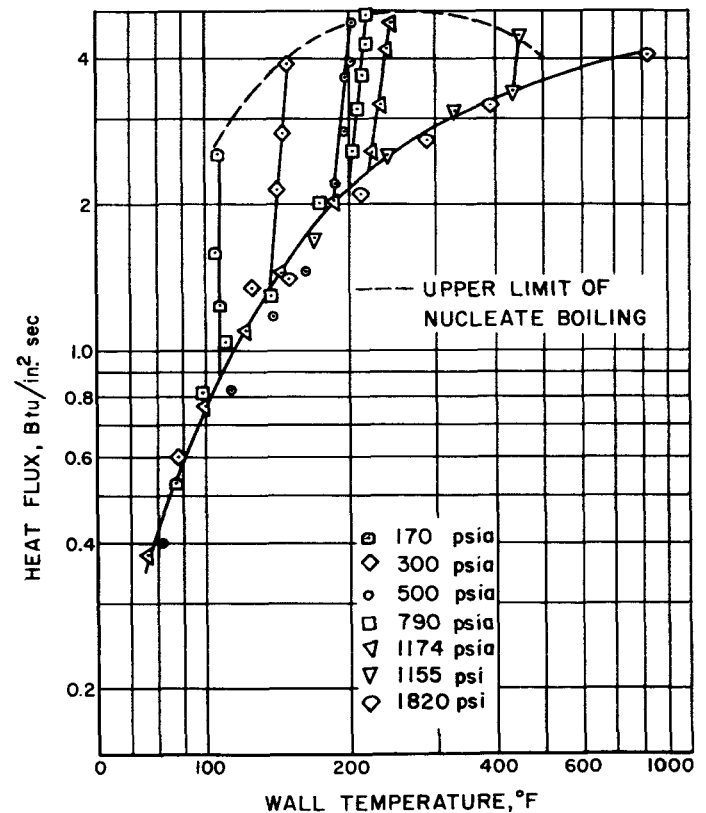Figure 6. Correlation of nonboiling forced-convection data with the Sieder–Tate equation

Figure 7. Heat flux as a function of wall temperature for a velocity of 30 ft/sec and an inlet liquid bulk temperature of 50°F
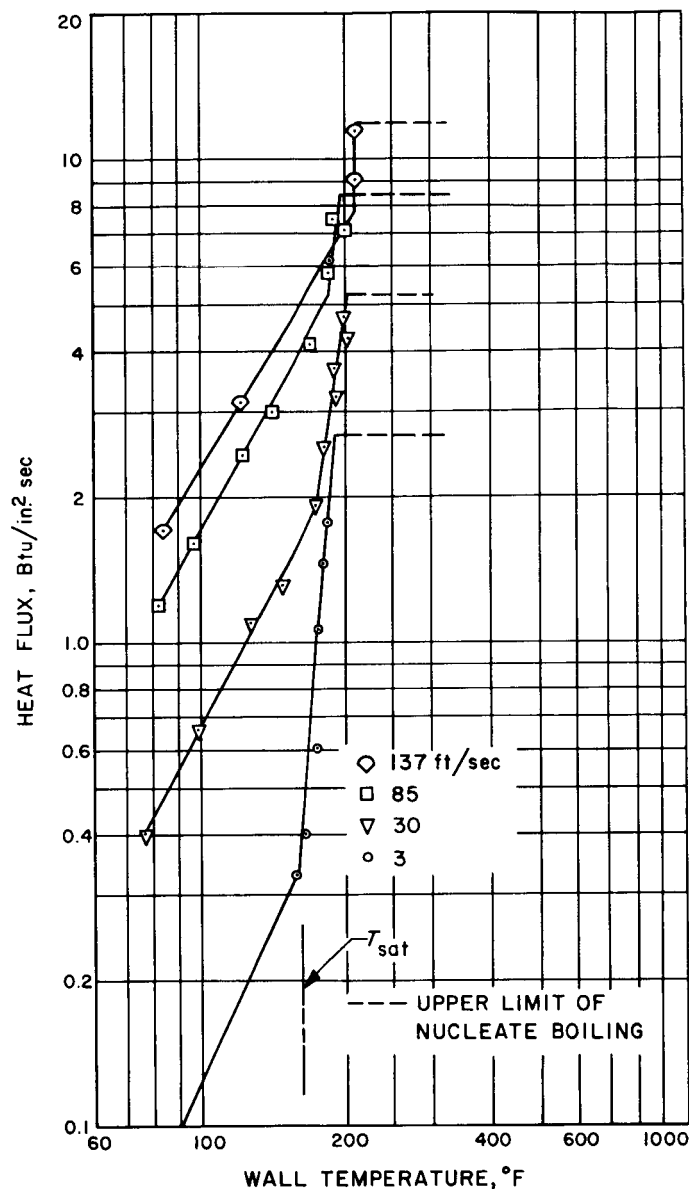
Figure 8. Heat flux as a function of wall temperature for a pressure of 500 psia and a bulk temperature of 55°F ± 5

Figure 9. Heat flux at the upper limit of nucleate boiling as a function of pressure
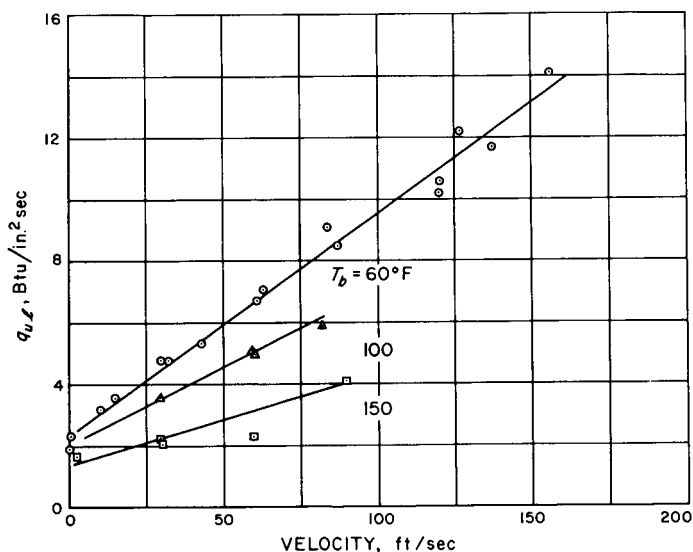
Figure 10. Heat flux at the upper limit of nucleate boiling as a function of velocity for various liquid bulk temperatures at a pressure of 500 psia

the inside wall temperature reaches a value somewhere between 0 and 60°F above the saturation temperature of the liquid (see Fig. 16), nucleate boiling commences. The magnitude of the difference between wall temperature and saturation temperature $(T_{wi} - T_{sat})$ at which nucleate boiling begins is dependent upon the test conditions. This temperature difference generally increases slightly as velocity is increased and is virtually unaffected by pressure and bulk temperature. These values of temperature difference are in general agreement with those found by other investigators (Ref. 7).

Wall temperatures are nearly constant in the nucleate-boiling region, varying less than 50°F between inception and the upper limit at given flow conditions. Wall temperatures can, therefore, be predicted by adding approximately 25°F to the saturation temperature. Fluid pressure is the only variable that substantially affects wall temperature under nucleate-boiling conditions because of the pressure effect on saturation temperature. Wall temperatures in the nucleate-boiling region, as well as in the non-boiling region, generally do not impose a design limit on rocket-engine thrust chambers; consequently, the suggested approximation for determining wall temperature is sufficiently accurate for practical considerations.

D. Upper Limit of Nucleate Boiling

The heat flux at the upper limit of nucleate boiling q_{ul} is of primary interest for the design of rocket-engine coolant passages because of the sudden large increase in wall temperature associated with the transition from nucleate boiling to film boiling. It was necessary to determine experimentally the relationship of q_{ul} to the variables p, V, and T_L, since no general method of predicting q_{ul} is available. During the tests the transition to film boiling under all test conditions, except those at 1000 psia and above, resulted in tube failure before the heat flux could be reduced. At these higher pressures, the heat-transfer coefficient of the vapor film is sufficient to support a heat flux at a wall temperature below failure limits. Therefore, the application of electrical power to the test section could be terminated before tube failure occurred.

In Fig. 9, q_{ul} is plotted vs pressure for given values of bulk temperature and velocity. At the two higher velocities shown (80 ft/sec and 30 ft/sec) the maximum value of q_{ul} was obtained at a pressure of about 900 psia, or approximately 55% of the critical pressure of 1657 psia. At zero velocity the peak value of q_{ul} was observed to occur at about 500 psia, or approximately 30% of critical pressure. Cichelli and Bonilla (Ref. 8) also found the peak value of q_{ul} for several liquids with zero velocity to be approximately 30% of the critical pressure of the fluid.
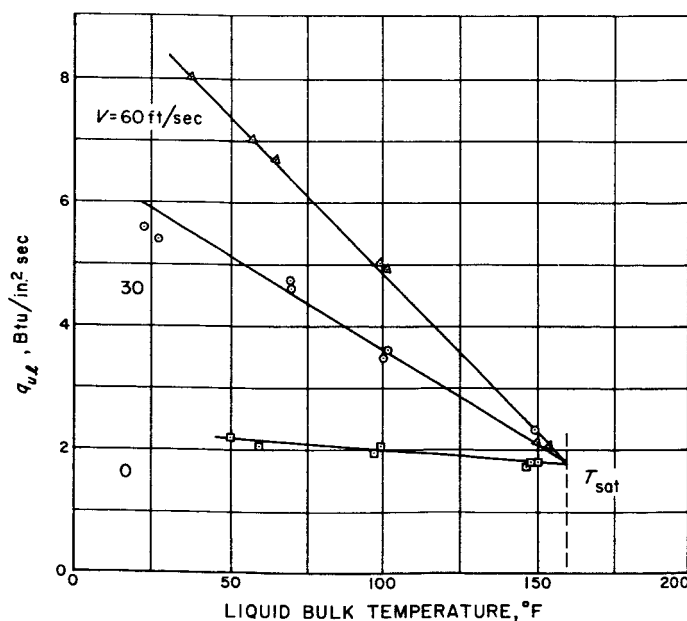

Figure 11. Heat flux at the upper limit of nucleate boiling as a function of liquid bulk temperature for various velocities at a pressure of 500 psia

Nucleate boiling cannot exist above the critical pressure. Therefore, the heat flux measured for the test at 1820 psi is not q_{ul} but a heat flux at which the wall temperature exceeded 700°F (see Fig. 7).

The effect of velocity on q_{ul} is shown in Fig. 10, where it may be observed that q_{ul} increases linearly with velocity. The slopes of the curves are found to be dependent on liquid bulk temperature.

Figure 11 shows the effect of liquid bulk temperature on values of q_{ul} for velocities of 0, 30, and 60 ft/sec at a pressure of 500 psi. Values of q_{ul} were found to decrease linearly with increasing bulk temperature to virtually a common value at the saturation temperature (160°F at a pressure of 500 psia). Bulk-temperature effects on q_{ul} are more pronounced at the higher velocities.

An interpolation equation has been derived for computing q_{ul} from the experimental results:

$$q_{ul} = \left[1 - 0.168 \left(\frac{p - 530}{530} \right)^2 \right] [1.85 + (0.0083 + 7.0 \times 10^{-4} V) \Delta t_{sub}]$$

(8)

The comparison of experimental values of q_{ul} with those obtained from Eq. 8 for the same conditions is shown in Fig. 17. Most of the experimental data lie within ±20% of this equation. It should be emphasized that Eq. 8 was established from the best fit of experimental data rather than from a fundamental heat-transfer consideration.

In Table 1 the experimental values of q_{ul} are listed for each condition of pressure, velocity, and bulk temperature tested.

E. Total Heat Load

The capability of a coolant to accept the total heat load of a given size engine is dependent upon its specific heat, the difference between saturation temperature and coolant inlet temperature to the thrust chamber, propellant mixture ratio, and propellant combination. Comparisons of various propellant combinations, including NH_3–RFNA and NH_3–O_2, for arbitrary given conditions of a 50,000-lb-thrust engine are shown in Ref. 1. The ability of the ammonia systems, using ammonia as the coolant, to accept the total heat load is marginal compared to some of the other systems, such as RFNA–UDMH with RFNA as the coolant, Corporal fuel–SFNA with Corporal

DATA (-□-,-●-) FROM *INDUSTRIAL AND ENGINEERING CHEMISTRY*, NOVEMBER, 1952, "VISCOSITY OF LIQUID AMMONIA AT HIGH PRESSURES" —L. T. CARMICHAEL AND B. H. SAGE (CIT)

-1000 psia

VALUES OF μ FOR $T > 190°F$ ARE FROM EXTRAPOLATED PORTION OF SIMILAR PLOT ON SEMILOG GRAPH PAPER

-BUBBLE POINT
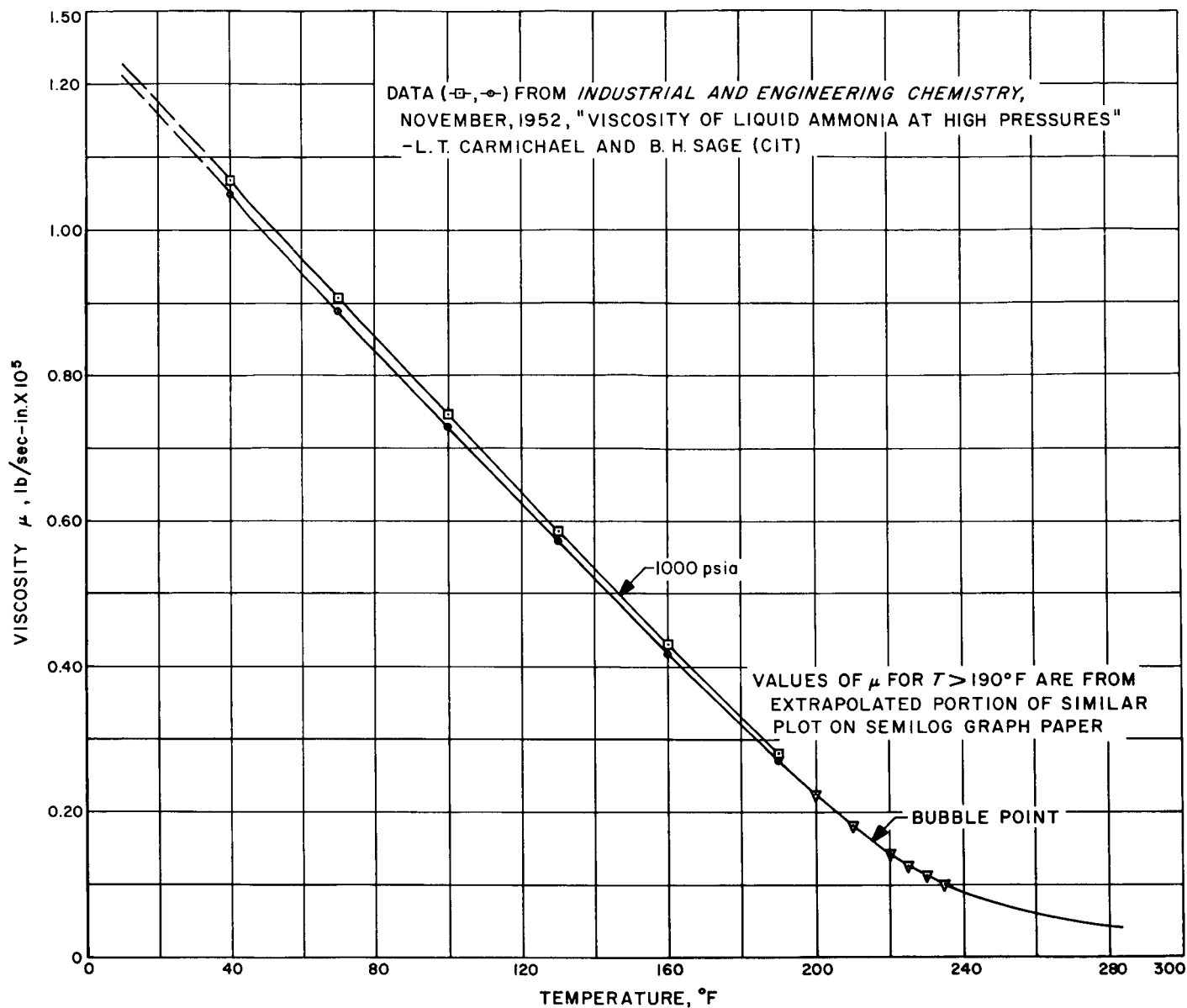
Figure 12. Viscosity of ammonia as a function of temperature and pressure

DATA FROM REF 10
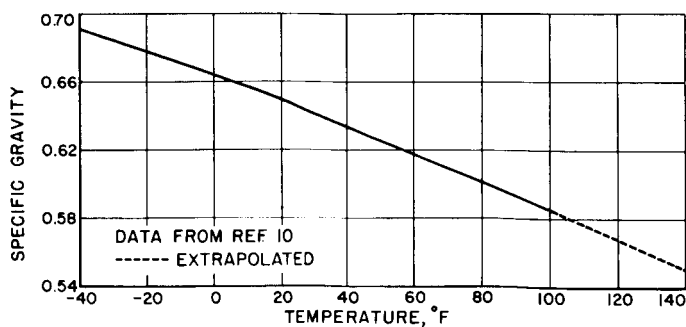------ EXTRAPOLATED

Figure 13. Specific gravity of ammonia as a function of temperature
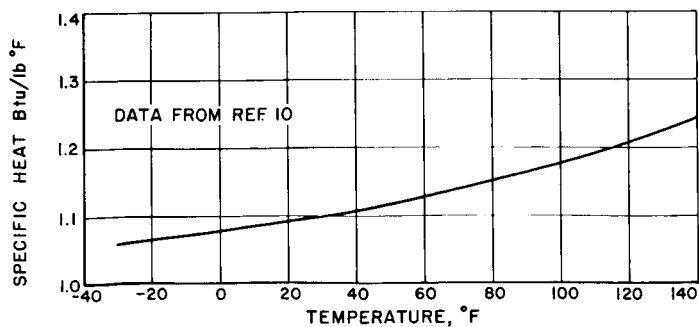

DATA FROM REF 10

Figure 14. Specific heat of ammonia as a function of temperature

fuel as the coolant, DETA–SFNA with DETA as the coolant, and JP-3–N₂O₄ with JP-3 as the coolant. It is of interest to note, however, that at a temperature of 100°F the specific heat of ammonia is 1.17 Btu/lb °F, which is high
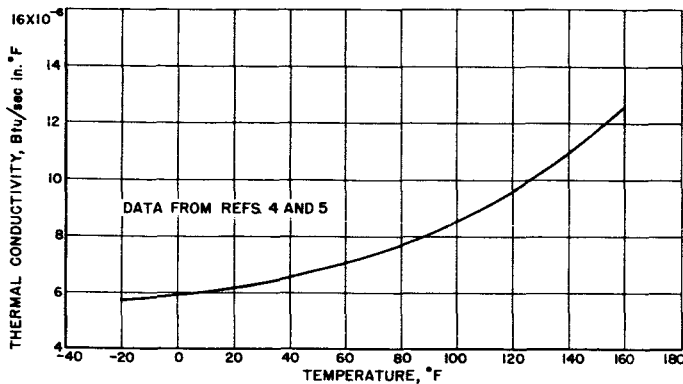

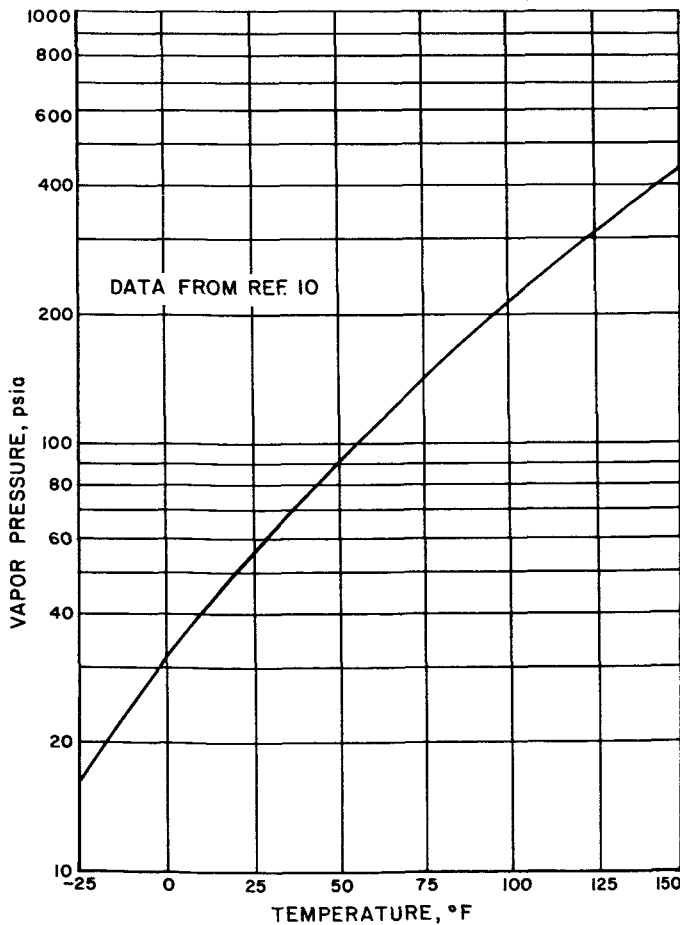**Figure 15. Thermal conductivity of ammonia as a function of temperature**

Figure 16. Vapor pressure of ammonia as a function of temperature

Table 1. Values of q_{ul}

Velocity ft/sec	Pressure psia	T_L (outlet) °F	q_{ul} Btu/in.² sec
32.0	495	22.5	5.64
31.6	500	27.5	5.38
30.0	500	76.0	4.76
30.0	494	100.5	3.41
30.0	490	101.0	3.50
30.0	478	149.0	2.29
29.5	504	152.0	2.08
30.0	170	66.0	2.53
30.0	170	62.0	2.32
30.0	300	67.0	3.88
32.5	540	76.5	4.72
30.0	794	80.0	4.95
31.1	954	67.0	5.58
32.9	1025	63.0	5.46
30.0	1174	77.0	4.77
25.4	1555	63.0	4.50
27.5	1820	75.0	4.11*
60.0	484	38.0	8.03
63.0	490	58.0	7.01
61.7	484	65.0	6.69
56.0	497	99.0	5.00
60.0	492	101.0	4.90
55.2	502	154.0	4.16
89.0	206	73.0	3.75
81.7	352	59.0	6.90
87.0	496	63.0	8.45
84.0	516	58.0	9.12
84.5	530	66.5	7.23
81.6	775	60.0	9.30
82.7	1005	61.0	9.52
80.6	1020	70.0	8.98
81.6	1215	68.0	8.96
3.0	494	158.0	1.73
3.0	504	140.0	2.41
10.0	499	75.0	3.12
15.2	486	71.0	3.52
42.2	518	77.0	5.36
82.3	504	108.0	5.82
97.2	518	65.5	8.29
98.5	500	124.5	3.42
121.0	500	53.5	10.60
124.0	500	57.5	10.21
127.5	475	67.5	12.20
137.0	516	58.0	11.64
156.0	500	65.0	14.30

*Heat flux at which the wall temperature exceeded 700°F.

compared to 0.42 Btu/lb °F for RFNA, 0.50 Btu/lb °F for Corporal fuel, 0.435 for JP-3, 0.393 for N₂O₄, and 0.744 for N₂H₄. The comparatively low saturation temperature of NH₃ imposes a restriction on its cooling capability and offsets the high specific heat.
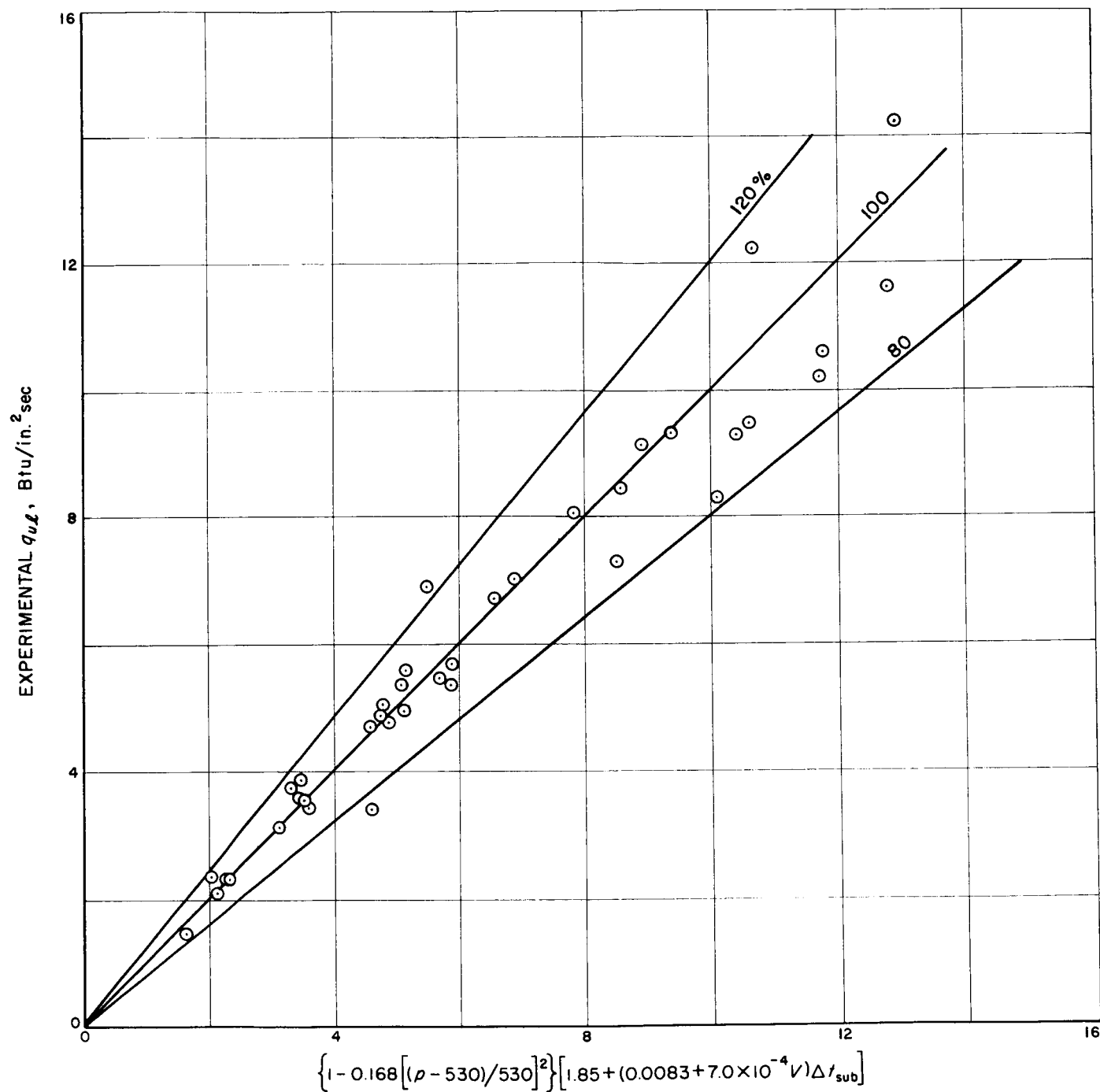
$$\left\{1-0.168\left[(p-530)/530\right]^{2}\right\}\left[1.85+(0.0083+7.0\times10^{-4}V)\Delta t_{sub}\right]$$

Figure 17. Comparison of experimental values
of q_{ul} with Eq. (8)

VII. CONCLUSIONS

The results from this experimental heat-transfer investigation showed that the convective heat-transfer coefficient of ammonia in the turbulent-flow nonboiling region could be predicted within ±20% by the Sieder–Tate equation when the physical properties were evaluated at the liquid-bulk temperature and a correction was made for the viscosity distribution across the boundary layer.

The wall temperature at the inception of nucleate boiling is equal to the saturation temperature plus about 25°F. Once nucleate boiling was established, the wall temperature remained nearly constant with increasing heat flux until q_{ul} was reached. Values of q_{ul} were reproducible and showed trends as a function of pressure, velocity, and liquid bulk temperature typical of other liquids. At a given pressure, the value of q_{ul} increased with increasing velocity and decreased with increasing bulk temperature to an apparent common value at the saturation temperature. As a function of pressure, values of q_{ul} were a maximum at about 55% of the critical pressure under flow conditions; whereas, at zero velocity, q_{ul} reached a maximum at about 30% of the critical pressure.

The capability of ammonia as a regenerative coolant for rocket engines is dependent upon its ability to accept local heat fluxes (which is established by q_{ul}) and its ability to accept total heat loads of the entire thrust chamber. For comparative purposes, the values of q_{ul} of various propellants are given at a pressure of 300 psia, a velocity of 30 ft/sec, and a liquid bulk temperature of 100°F; they are 2.5 for NH_3, 4.5 for JP_3, 4.6 for N_2O_4, 6.8 for RFNA, 8.1 for Corporal fuel, and 12.4 for N_2H_4. Consequently, the local cooling capability of ammonia at these conditions is comparatively low. The total heat-load cooling capability of NH_3 is limited by the low saturation temperature, even though it has a high specific heat value.

NOMENCLATURE

A area, in.^{2}

c_p specific heat at constant pressure, Btu/lb °F

D diameter of tube, in.

E voltage, v

h heat-transfer coefficient, Btu/sec in.^{2} °F

I current, amp

k thermal conductivity, Btu/sec in. °F, except as noted

L length of test section, in.

M molecular weight

Nu Nusselt number $= \dfrac{h D_i}{k}$ (dimensionless)

Pr Prandtl number $= \dfrac{\mu c_p}{k}$ (dimensionless)

q heat flux, Btu/in.^{2} sec

r radius, in.

R resistance, Ω

Re Reynolds number $= \dfrac{\rho D_i V}{\mu}$ (dimensionless)

S specific gravity

T temperature, °F

t wall thickness, in.

v velocity, ft/sec

$\dot{w}$ weight flow rate, lb/sec

ΔT temperature difference, °F

μ viscosity, lb/in. sec, except as noted

ρ density, lb/in.^{3}

NOMENCLATURE (Cont'd)

Subscripts

b liquid bulk condition

i inner

o outer

s surface normal to heat flow

sat saturation condition

sub subcooling (i.e., saturation condition minus bulk condition)

ul upper limit of nucleate boiling

w wall condition

REFERENCES

1. Bartz, D. R., *Factors Which Influence the Suitability of Liquid Propellants as Rocket Motor Regenerative Coolants,* Memo No. 20-139, Jet Propulsion Laboratory, Pasadena, December 28, 1956.

2. Massier, P. F., *A Forced Convection and Nucleate Boiling Heat-Transfer Test Apparatus,* Technical Report No. 32-47, Jet Propulsion Laboratory, Pasadena, February 3, 1961.

3. McAdams, W. H., *Heat Transmission,* McGraw Hill Book Co., Chapter VII, p. 168, 1942.

4. Perry, John H., *Chemical Engineers' Handbook,* Second Edition, 1941, p. 962.

5. Kardos, A., "Die Wärmenleitfähigkeit verschiedener Flüssigkeiten," *Zeitschrift für die gesamte Kälte-Industrie,* Vol. 41, No. 2 (1934).

6. Hartnett, J. P., "Experimental Determination of the Thermal-Entrance Length for the Flow of Water and of Oil in Circular Pipes," *ASME Transactions,* Vol. 77, p. 1211, November 1955.

7. Reinhardt, T. F., Potter, R. L., and Moore, F. M., "Heat Transfer Properties of Anhydrous Ammonia," *OASD Research and Development,* p. 85, Liquid Propellants Symposium, March 27–28, 1957.

8. Cichelli, M. T., and Bonilla, C. F., *Transactions of the American Institute of Chemical Engineers,* Vol. 41, p. 755, 1945.

9. Carmichael, L. T., and Sage, B. H., "Viscosity of Liquid Ammonia at High Pressure," *Industrial and Engineering Chemistry,* Vol. 44, Pt. II, pp. 2728–32, 1952.

10. *Tables of Thermodynamic Properties of Ammonia,* National Bureau of Standards Circular No. 142, April 19, 1923.